Check for updates

Received: 30 August 2021 | Revised: 20 October 2021 | Accepted: 22 October 2021

DOI: 10.1002/ppap.202100151

RESEARCH ARTICLE

PLASMA PROCESSES AND POLYMERS

Toward defining plasma treatment dose: The role of plasma treatment energy of pulsed-dielectric barrier discharge in dictating in vitro biological responses

Abraham Lin[1,2] | **Eline Biscop**[1,2] | **Yury Gorbanev**[1] | **Evelien Smits**[2] | **Annemie Bogaerts**[1]

[1]PLASMANT-Research Group, University of Antwerp, Antwerp, Belgium

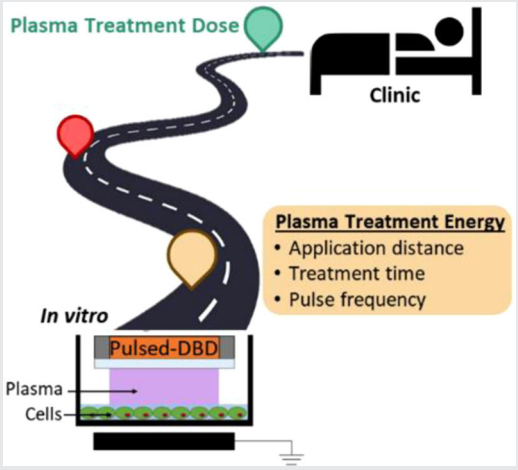
[2]Center for Oncological Research—Integrated Personalized & Precision Oncology Network (IPPON), University of Antwerp, Antwerp, Belgium

Correspondence
Abraham Lin, PLASMANT-Research Group, University of Antwerp, PLASMANT Lab Universiteitsplein 1, Antwerp 2610, Belgium.
Email: Abraham.lin@uantwerpen.be

Funding information
Fonds Wetenschappelijk Onderzoek, Grant/Award Numbers: 12S9218N, 12S9221N, G044420N

Abstract

The energy dependence of a pulsed-dielectric barrier discharge (DBD) plasma treatment on chemical species production and biological responses was investigated. We hypothesized that the total plasma energy delivered during treatment encompasses the influence of major application parameters. A microsecond-pulsed DBD system was used to treat three different cancer cell lines and cell viability was analyzed. The energy per pulse was measured and the total plasma treatment energy was controlled by adjusting the pulse frequency, treatment time, and application distance. Our data suggest that the delivered plasma energy plays a predominant role in stimulating a biological response in vitro. This study aids in developing steps toward defining a plasma treatment unit and treatment dose for biomedical and clinical research.



KEYWORDS
cancer treatment, non-thermal plasma, plasma energy, plasma medicine, plasma treatment dose

1 | INTRODUCTION

Non-equilibrium, atmospheric pressure plasma technologies are continually being investigated for biomedical applications, including hemostasis,[1,2] wound healing,[3,4] dentistry,[5] surface sterilization,[6] neuroregeneration,[7,8] and cancer therapy.[9–11] These technologies are commonly referred to as cold atmospheric plasma or non-thermal plasma (NTP) in the biomedical and clinical fields. The extensive range of reported plasma-induced biological effects has been attributed to the reactive oxygen and nitrogen species (RONS) generated by plasma[12–15] as well as the cellular phenomena, hormesis.[16] Hormesis emphasizes the dose dependence of an agent to have either a beneficial or

 © 2021 Wiley-VCH GmbH
https://doi.org/10.1002/ppap.202100151

16128869, 2022, 3, Downloaded from https://onlinelibrary.wiley.com/doi/10.1002/ppap.202100151 by Universiteit Antwerpen, Wiley Online Library on [23/12/2022]. See the Terms and Conditions (https://onlinelibrary.wiley.com/terms-and-conditions) on Wiley Online Library for rules of use; OA articles are governed by the applicable Creative Commons License

detrimental biological effect. In the context of plasma treatment, this suggests that low-dose plasma treatment could promote regenerative effects, while higher dose treatments could induce cytotoxicity.[16] Therefore, based on the medical application (e.g., wound healing, cancer treatment), it is critical to define the appropriate plasma treatment dose.[16,17]

To date, an appropriate plasma treatment unit has not been defined or standardized in the field of plasma medicine. A major challenge has been the plethora of plasma devices, setups, and settings currently in use. Over the years, two main classes of plasma devices have emerged as the predominantly used systems for biomedical applications: the pulsed-dielectric barrier discharge (DBD) and the plasma jet.[18,19] Although there have been comparative studies of pulsed-DBD and plasma jet treatments for a predefined cellular response,[20] a unifying dose parameter remains elusive due to the different configurations and dependencies of the systems, which subsequently affect RONS generation and delivery (Table 1). While both DBDs and plasma jets also produce varying degrees of low-level ultraviolet radiation and electric fields that can be affected by these parameters, it has been reported that these plasma components alone have negligible contributions to biological effects compared to the chemical species produced.[21–23] Therefore, identifying the major contributing parameters of these different plasma systems would be a major step toward defining plasma treatment dose.

Recently, our group has investigated the interaction mechanism of a microsecond-pulsed DBD plasma with cancerous cells. We determined a regime of plasma that induced immunogenic cancer cell death,[24] an attractive type of cell death for cancer immunotherapy.[25] A thorough examination of the RONS generated by the microsecond-pulsed DBD plasma was also performed, showing that the short-lived species (e.g., $^{\bullet}OH$, $^{\bullet}NO$, O/O_3) were most responsible for inducing cell death and increasing cancer immunogenicity.[24] Furthermore, we observed that the generation of RONS with the DBD plasma system increased linearly with pulse frequency or treatment time when the other parameters were fixed. Taken together, we hypothesized that the plasma treatment energy encompasses the major influence of application parameters (Table 1; e.g., pulse frequency, duration, distance) for pulsed-DBD treatment and dictates in vitro biological response.

In the present study, we investigated the energy dependence of pulsed-DBD plasma treatment on RONS generation and biological response, specifically for cancer cell treatment. We measured the plasma power in a setting that closely resembles in vitro biological experiments to determine the energy delivered per plasma pulse during treatment. The total energy of treatment was calculated based on the energy per pulse and the total number of delivered pulses. At higher treatment distances, the energy per pulse was reduced, so treatment time was increased to deliver the same plasma energy. Chemical measurements of RONS and biological analysis on three different cell lines were performed at a fixed treatment energy, while other parameters were adjusted. Our results showed that when pulsed-DBD plasma treatment energy was fixed, an equivalent level of cancer cell survival was achieved, regardless of changes to several other parameters. This was similarly observed for the amount of RONS generated. Taken together, our data suggest that the plasma treatment energy encompasses the influence of major pulsed-DBD application parameters and dictates in vitro biological response. This has major implications toward defining a standardized plasma treatment unit and treatment dose for biomedical applications.

TABLE 1 Parameters that influence dielectric barrier discharge (DBD) and plasma jet treatment

Parameters	Pulsed-DBD	Plasma jet
Electrical	Waveform, voltage	Waveform, voltage
Application	Pulse frequency, duration, distance	Pulse frequency, duration, distance, flow rate
Environmental	Atmospheric gas composition, Humidity, Treatment surface	Feed gas, Humidity, Treatment surface

2 | EXPERIMENTAL SECTION

2.1 | Experimental design

We hypothesized that the total plasma energy delivered during treatment encompasses the influence of major application parameters and dictates the production of chemical species and biological effects in vitro.

The aim of this study was to investigate the importance of application parameters individually (i.e., application distance, pulse frequency, treatment time) and plasma treatment energy collectively on biological responses and generated chemical species. This was accomplished by (1) determining the energy per pulse of the DBD plasma during the treatment of biological samples, (2) analyzing cancer cell survival, and (3) measuring chemical species in liquid.

16128869, 2022, 3, Downloaded from https://onlinelibrary.wiley.com/doi/10.1002/ppap.202100151 by Universiteit Antwerpen, Wiley Online Library on [23/12/2022]. See the Terms and Conditions (https://onlinelibrary.wiley.com/terms-and-conditions) on Wiley Online Library for rules of use; OA articles are governed by the applicable Creative Commons License

2.2 | Microsecond-pulsed power supply

A microsecond-pulsed DBD plasma system was chosen for this study, unless otherwise specified, based on our previous experience with this system for cancer treatment.[26] The power supply was custom built (Megaimpulse Ltd.), producing a 2-μs pulse (~30 kV) with a rise time of 1—1.5 μs. This system has been shown to be effective for the treatment of three-dimensional tumors in vitro and in vivo.[26] Power measurements were performed on this DBD plasma system and liquid chemistry and cell survival analysis were also performed to determine the effects of different plasma application parameters (i.e., pulse frequency, treatment time, application distance, and total energy). The output of the power supply was connected to a DBD electrode. This copper electrode (1.5 cm diameter) was covered with a 0.5-mm fused silica dielectric with a diameter of 1.2 cm (Technical Glass).

2.3 | Power measurements

To determine the plasma power during treatment of cells in vitro, voltage and current were measured (Figure 1a) when plasma was generated at 500 Hz between the DBD electrode and a six-well plate on a grounded metal platform, to simulate the treatment of biological samples (Figure 1b). While all experiments were carried out in a 24-well plate, power measurements were performed in a six-well plate for ease of use. As all cell culture well plates from Corning have the same bottom thickness of 1.27 mm, which would serve as an additional dielectric, the discharge was not affected by different plate formats. The DBD system and electrodes were made with the intention of performing in vivo and clinical experiments, and therefore, they were made to be maximally insulating from the operator and treatment subject. Further manipulation of this setup would compromise the integrity of the shielding and introduce potential safety risks, so we had to perform power measurements using external voltage and current monitors. The position of the electrode was fixed with a z-positioner. Voltage was measured with a 1000× high-voltage probe (P6015A; Tektronix) and current was measured using a current monitor (4100; Pearson Electronics, Inc.). The voltage and current waveforms were recorded on an oscilloscope (DSOX1102G; Keysight) with a 50-ns sampling rate and averaging 64 pulses. Instantaneous power ($P(t)$) was determined from voltage and current: $P(t) = \mathrm{V}(t) \times I(t)$. Energy per pulse ($\varepsilon_{\mathrm{pulse}}$) is defined as the integration of the instantaneous power over the period of the pulse (T): $\varepsilon_{\mathrm{pulse}} = \int_0^T P(t)dt$. Therefore, we calculated the energy per pulse: $\varepsilon_{\mathrm{pulse}} = \sum_{k=1}^{n} |\mathrm{V}_k(t) \times \mathrm{I}_k(t)| \times \Delta t$, where Δt was 50 ns and the number of recorded samples (n) was 2000. Furthermore, the energy per pulse from displacement current was measured when the high-voltage pulse was applied to the DBD electrode without a surface to discharge on (30 mm above the bottom of the well). This value was subtracted from all energy measurements to account for the contribution of displacement current. Taken together, the energy per pulse reported here($\varepsilon_{\mathrm{pulse}}$) is the energy per pulse of the measured discharge $\varepsilon_{\mathrm{pulse(discharge)}}$ minus that of the displacement current $\varepsilon_{\mathrm{pulse(displacement)}}$:

$$\varepsilon_{\mathrm{pulse}} = \varepsilon_{\mathrm{pulse(discharge)}} - \varepsilon_{\mathrm{pulse(displacement)}}. \quad (1)$$

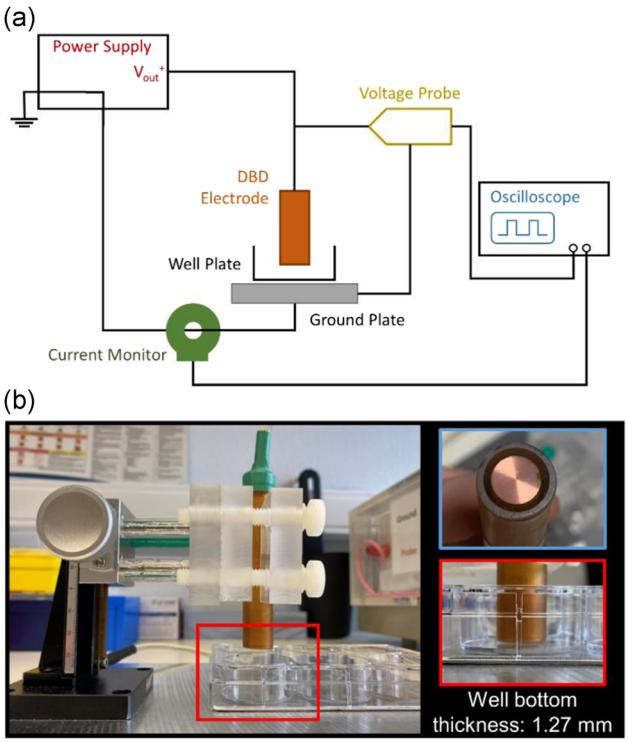


FIGURE 1 Experimental setup. (a) A schematic of the experimental setup to measure pulsed-dielectric barrier discharge (DBD) plasma power is shown. (b) A z-positioner was used to fix the position of the DBD electrode (blue insert) above the well for plasma treatment (red insert)

2.4 | Chemical measurements

The microsecond-pulsed DBD was used to treat 50 μl of phosphate-buffered saline (PBS) solution in a 24-well plate. The DBD electrode was positioned 1 mm above the liquid and plasma was generated in direct contact at varying pulse frequencies and treatment times. Following treatment, PBS was immediately collected and

16128869, 2022, 3, Downloaded from https://onlinelibrary.wiley.com/doi/10.1002/ppap.202100151 by Universiteit Antwerpen, Wiley Online Library on [23/12/2022]. See the Terms and Conditions (https://onlinelibrary.wiley.com/terms-and-conditions) on Wiley Online Library for rules of use; OA articles are governed by the applicable Creative Commons License

analyzed for specific RONS. All chemical measurements were performed with at least three repeats on the same day.

2.4.1 | H_2O_2 measurements

A fluorometric assay kit (MAK165; Merck) was used according to the manufacturer's instructions to measure the H_2O_2 concentration. As performed in our previous work,[27] 25 µl of PBS treated with DBD plasma was added to each well and diluted with an equal amount of untreated PBS for a final volume of 50 µl. A master mix containing 4.75 ml of assay buffer + 50 µl red peroxidase substrate + 200 µl 20 units/ml peroxidase was then added to each well (50 µl), and samples were incubated for 30 min. Fluorescence was measured using the Tecan Spark Cyto (λex: 540 ± 20 nm, λem: 590 ± 20 nm, fixed gain: 44).

2.4.2 | NO_2^- and NO_3^- measurements

A NO_2^-/NO_3^- colorimetric assay kit (780001; Cayman Chemical) was used for these experiments following the developed protocols. NO_2^- was detected by adding 50 µl of Griess reagent 1 (sulfanilamide) to the DBD plasma-treated PBS in a 96-well plate, followed by immediate addition of 50 µl of Griess reagent 2 (*N*-(1-naphthyl) ethylenediamine). To measure both NO_2^- and NO_3^- ($NO_2^- + NO_3^-$), a nitrate reductase mixture (780010; Cayman Chemical) and an enzyme cofactor mixture (780012; Cayman Chemical) were added to each sample and incubated for 1 h before the Griess reagent steps, thus allowing for the conversion of NO_3^- into NO_2^-. Due to the assay protocol and the small volumes treated, the concentrations of NO_2^- and NO_3^- were measured from independent experiments. An estimate of NO_3^- concentrations was, therefore, calculated by subtracting the mean NO_2^- concentration of each treatment condition from the $NO_2^- + NO_3^-$ concentrations. Samples were prepared in triplicate and the absorbance wavelength was measured at 540 nm using a Tecan Spark Cyto (20 readings per well). Concentrations of NO_3^- and NO_2^- were calculated from a calibration curve, obtained using standard solutions provided in the assay kit.

2.5 | Biological analysis

The microsecond-pulsed DBD was used to treat three cancer cell lines seeded in 24-well plates. Medium in the well was removed right before treatment and the DBD electrode was positioned above the cells. Plasma was generated in direct contact with the cells at varying distances, pulse frequencies, and treatment times, and the fresh medium was replenished immediately after treatment.

2.5.1 | Cell culture and treatment

A melanoma cell line (A375), a squamous cell carcinoma cell line (CAL-27) and a glioblastoma cell line (U87) were used in this experiment as they originate from different tissues, thus providing a broad overview of pulsed-DBD plasma effects without limitation to a single cancer type. All cell lines were cultured in Dulbecco's modified Eagle medium containing 10% fetal bovine serum, 100 U ml^{-1} penicillin, and 100 µl of streptomycin. The melanoma media contained 4×10^{-3} M L-glutamine, while the other cell line media contained 2×10^{-3} M L-glutamine. All cells were cultured in a humidified environment at 37°C with 5% CO_2 and plated in 24-well plates (150 000 cells/well) 1 day before DBD plasma treatment. The medium was removed from the well right before treatment and the DBD electrode was lowered into the well and fixed at a position using a z-positioner (Figure 1b). Plasma was then discharged directly on the cells at parameters defined for each experiment. Following treatment, 500 µl of fresh medium was immediately replenished in the well and cells were immediately analyzed.

2.5.2 | Cell survival assay

Cell survival was quantified immediately after DBD plasma treatment using the Trypan Blue exclusion test. Cell supernatant was collected from the wells and the cells were washed with 200 µl of PBS. The PBS was also collected with the cell supernatant and 200 µl of Accutase was added to each well to detach the cells. The cell suspension, supernatant, and PBS wash were pooled together for each well and homogenized. In this way, all the cells were collected after DBD plasma treatment and 20 µl of this cell suspension was acquired for cell counting. An equal part of 0.4% Trypan Blue (15250-061; Gibco) was added to each sample and counts were performed on an automated cell counter (TC20 Automated Cell Counter; Bio-Rad). Live cell concentrations were recorded, and survival reported here was a normalization of live cell counts to that of the untreated controls.

2.6 | Statistical analysis

Statistical differences for cell survival were analyzed using JMP Pro 13 (SAS software) using the linear mixed

16128869, 2022, 3, Downloaded from https://onlinelibrary.wiley.com/doi/10.1002/ppap.202100151 by Universiteit Antwerpen, Wiley Online Library on [23/12/2022]. See the Terms and Conditions (https://onlinelibrary.wiley.com/terms-and-conditions) on Wiley Online Library for rules of use; OA articles are governed by the applicable Creative Commons License

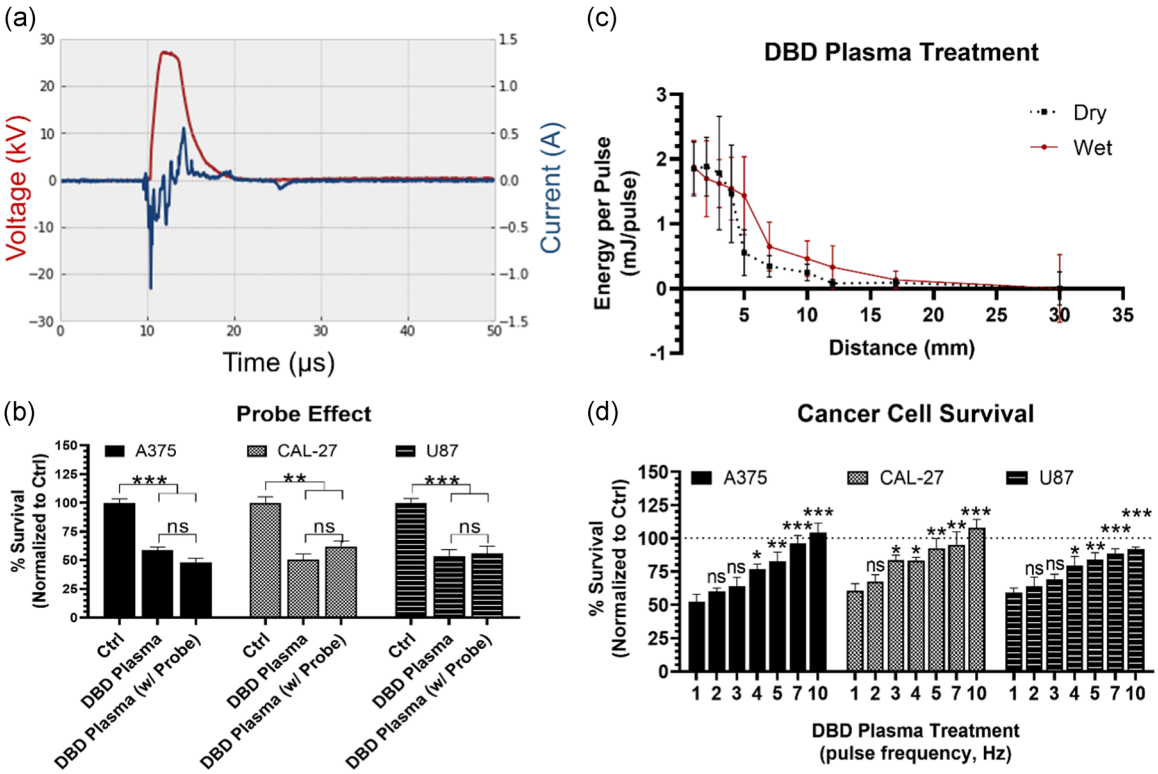


FIGURE 2 Electrical characterization of the dpulsed-DBD plasma system. (a) Voltage and current waveform of a single DBD plasma discharge in a six-well plate was measured on the oscilloscope. (b) To determine if the attachment of the voltage probe significantly affected plasma power, the effect of plasma treatment on cancer cell survival was compared with and without the probe. DBD plasma treatment significantly reduced the cell survival of three cancer cell lines (melanoma, A375; squamous cell carcinoma, CAL-27; glioblastoma, U87) and no statistical difference was measured with and without the probe connected to the system ($n = 3$–6). Treatment conditions were compared to each other to determine statistical significance. $^{ns}p \geq 0.05$; $^{**}p \leq 0.01$; $^{***}p \leq 0.001$ (generalized linear mixed model, Tukey's test). (c) The energy per pulse was calculated from the voltage and current waveform (see text) at different application distances for a dry and wet well. (d) These results were correlated to cancer cell survival after treatment when the cells were exposed to DBD plasma at varying distances. All treatment conditions were compared to that of the 1 mm application distance to determine statistical significance ($n = 3$–7). Data are represented here as mean ± SEM. ns, not significant. $^{ns}p \geq 0.05$; $^{*}p \leq 0.05$; $^{**}p \leq 0.01$; $^{***}p \leq 0.001$ (generalized linear mixed model, Dunnett's test)

model with treatment as the fixed effect. When the difference was significant ($p \leq 0.05$), an adjusted p value was calculated using Dunnett's test when comparing to one group (e.g., untreated controls, 1 mm application distance) or Tukey's test when comparing all conditions to each other. Measurements were performed on the same day for each chemical species, in at least triplicate. All in vitro experiments were performed in at least triplicates and repeated on separate days as independent replicates. For both in vitro experiments and chemical measurements, the total number of observations (n) is defined in the figure legend. Nonlinear regression using the least-squares regression was performed for the chemical species measurements to determine linearity using GraphPad Prism (GraphPad Software). The voltage and current plots were prepared using Python and all other figures were prepared in GraphPad Prism (GraphPad Software). Data are represented as mean ± standard error of the mean for in vitro experiments and mean ± standard deviation for chemical measurements.

3 | RESULTS

3.1 | Energy per pulse of DBD plasma

The energy of a single DBD discharge was calculated based on voltage and current measurements (Figure 2a) and after accounting for displacement current (details in Section 2). As the physical and electrical properties of a material can affect the discharge characteristics of the plasma in contact with it,[28] we measured the energy per pulse in an environment that most closely resembles the treatment of biological samples. The DBD electrode was lowered into the well of a six-well plate (polystyrene; 1.27 mm bottom thickness) and positioned 1 mm above the bottom, a

16128869, 2022, 3, Downloaded from https://onlinelibrary.wiley.com/doi/10.1002/ppap.202100151 by Universiteit Antwerpen, Wiley Online Library on [23/12/2022]. See the Terms and Conditions (https://onlinelibrary.wiley.com/terms-and-conditions) on Wiley Online Library for rules of use; OA articles are governed by the applicable Creative Commons License

commonly used position for DBD treatment in vitro. As treatment of cells in vitro is never performed on dry samples, PBS was added into the well and then removed. Both the dry well and the wet well (PBS added and removed before discharge) conditions were tested. As commercial polystyrene cell culture plates are processed to be hydrophilic, which facilitates cell attachment, the PBS in the wet well appears to spread evenly along the bottom of the well and no visible aggregates were seen (Figure S1).

The energy per pulse for the wet and dry conditions was found to be 1.88 and 1.85 mJ/pulse, respectively, though they were not statistically different. As the addition of the voltage probe could also affect the plasma energy, we tested whether this would have an effect on the biological response. A melanoma (A375), a head and neck squamous cell carcinoma (CAL-27), and a glioblastoma (U87) cell line were treated with the DBD plasma at 500 Hz for 10 s. The medium was removed immediately before treatment and the DBD electrode was placed 1 mm above the cells. Plasma treatment was performed both without and with the voltage probe attached to the system and cancer cell survival was measured. DBD treatment reduced the survival of all three human cell lines and the attachment of the probe did not significantly affect treatment (Figure 2b). Therefore, we concluded that the probe did not significantly change the measured plasma energy and at 1 mm treatment, the discharge was ~1.88 mJ/pulse.

As the application distance of the DBD electrode would change the applied electric field and thus potentially affect the power of the discharge, we investigated the distance dependence of the energy per pulse. The energy per pulse for both the wet and dry treatment conditions was similar for distances up to 4 mm (Figure 2c). At 5 mm, we observed a decreasing trend, which was greater for the dry condition (0.56 ± 0.36 mJ/pulse) compared to the wet condition (1.44 ± 0.60 mJ/pulse), though this was not statistically significant. As the distance increased, the average energy per pulse continued to decrease, but it appears that at relatively small application distances ($\leq$4 mm), the energy per pulse is approximately the same.

To test the influence of application distance during DBD plasma treatment on the biological outcome, we treated the three human cancer cell lines with fixed plasma parameters (pulse frequency: 500 Hz; treatment time: 10 s) over a range of distances and measured cell survival. Cell survival for all treatment conditions was compared to that of 1 mm application distance within the cell lines. Between 1 and 2 mm application distance, DBD plasma treatment did not significantly change cancer cell survival (Figure 2d). Cell survival deviated from that of the 1 mm treatment condition at 3 mm for CAL-27 and 4 mm for A375 and U87. For all cell lines, it was clear that at distances 4 mm and greater, cell survival was significantly affected, and by 10 mm, DBD plasma treatment had no effect on survival. This is most likely due to the decrease in the applied electric field as a result of the larger air gap, and consequently, a lowering of plasma treatment energy. Taken together, the biological results shown here (Figure 2d), complement the electrical characterization of the DBD power supply (Figure 2c). For biological applications, in vitro, in vivo,[29–31] and especially in the clinic,[32–34] DBD plasma treatment is normally applied in close proximity to the target (1–2 mm) and, therefore, subsequent experiments were performed with 1 mm distances unless otherwise specified.

3.2 | Energy dependence of DBD plasma treatment on cancer cell survival

It is well documented that increasing plasma treatment duration or pulse frequency (particularly for direct pulsed-DBD plasma treatments) induces higher levels of cancer cell death.[21,24] This was also demonstrated with our DBD plasma system (Figure S2). Here, we tested our hypothesis that cancer cell death is dependent on the delivered plasma treatment energy and independent of a single parameter. The three cancer cell lines were exposed to DBD plasma, at a 1-mm distance, with a range of pulse frequencies (50—500 Hz) and application times (100—10 s). The number of delivered pulses was the same (5000 pulses) and the total delivered energy was calculated to be approximately 9.4 J based on the measured energy per pulse (Figure 1c).

Immediately after DBD plasma treatment, cells (and their supernatants) were collected, analyzed, and normalized to that of the untreated controls to obtain the percentage of cancer cell survival. DBD plasma treatment at 9.4 J reduced survival for all cell lines: $49\% \pm 3\%$ for A375, $59\% \pm 5\%$ for CAL-27, and $62\% \pm 2\%$ for U87. Furthermore, no significant difference was measured between the different treatment times and pulse frequencies (Figure 3a). Interestingly, a similar response was demonstrated using a second microsecond-pulsed DBD plasma system (details in the Supporting Information). Following exposure to plasma at an equivalent energy, two melanoma cell lines showed an increased immunogenicity marker and no difference was measured between the different conditions (i.e., pulse frequencies and treatment times) when the delivered plasma energy was held constant (Figure S3). Taken together, these results highlight the importance of plasma treatment energy for anticancer activity.

16128869, 2022, 3, Downloaded from https://onlinelibrary.wiley.com/doi/10.1002/ppap.202100151 by Universiteit Antwerpen, Wiley Online Library on [23/12/2022]. See the Terms and Conditions (https://onlinelibrary.wiley.com/terms-and-conditions) on Wiley Online Library for rules of use; OA articles are governed by the applicable Creative Commons License

Because both, energy per pulse and cancer cell death, decreased with application distance (Figure 2c,d), we also test our hypothesis that cell survival was dependent on the plasma treatment energy by treating the three cancer cell lines at various distances while delivering equivalent energies. The pulse frequency of DBD plasma treatment was fixed at 500 Hz, the application distance was fixed at either 1, 5, 7, or 10 mm, and the treatment time was adjusted to 10, 13, 30, and 41 s, respectively, to deliver a total of 9.4 J, based on the energy measured in the wet condition (Figure 2c). The energies per pulse at different distances are detailed in the figure. Regardless of time and distance, when the NTP treatment energy was fixed to 9.4 J, equivalent cell survival was achieved between the treatment groups of all three cell lines (Figure 3b). While all treatments were able to reduce cell survival to 60% ± 4% (A375), 65% ± 2% (CAL-27), and 58% ± 3% (U87) compared to untreated controls, no differences were measured between treatments at different heights.

Therefore, we demonstrated that equivalent cell survival could be achieved when the delivered plasma treatment energy was the same, regardless of the pulse frequency, treatment time, and application distance alone (Figure 3). Taken together, this strongly evidences the importance of pulsed-DBD plasma treatment energy in eliciting cell death over a single application parameter.

3.3 | Energy dependence of DBD plasma treatment for generating RONS

It is well documented that plasma-generated RONS are the major effectors of biological response.[13,16,21,24] Therefore, we also investigated how pulse frequency,

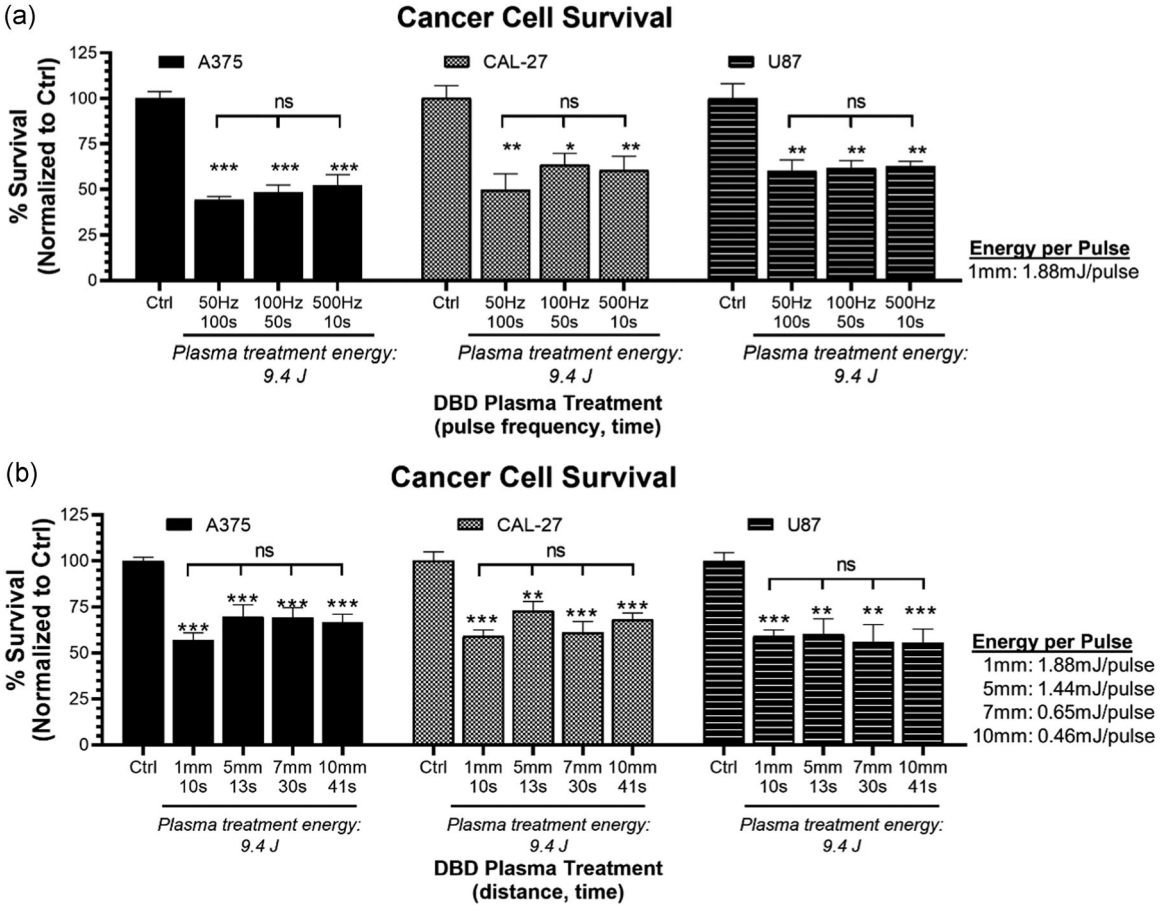


FIGURE 3 Energy dependence of pulsed-DBD plasma treatment for cancer cell survival. (a) Melanoma (A375), squamous cell carcinoma (CAL-27), and glioblastoma (U87) cells were exposed to 9.4 J of DBD plasma while varying the pulse frequency and the treatment duration ($n = 3$–6). While all treatment conditions resulted in a significant decrease in percent survival compared to untreated controls, no difference was observed between the different conditions. (b) The treatment time was extended at higher application distances, based on the drop in the energy per pulse, to deliver the same plasma treatment energy (9.4 J) to the cancer cells ($n = 5$–12). While all treatments reduced cell viability compared to untreated controls, no differences were observed between treatments. Treatment conditions were compared to each other to determine statistical significance. Data are represented here as mean ± SEM. ns, not significant. $^{ns}p \geq 0.05$; $^{**}p \leq 0.01$; $^{***}p \leq 0.001$ (generalized linear mixed model, Tukey's test)

16128869, 2022, 3, Downloaded from https://onlinelibrary.wiley.com/doi/10.1002/ppap.202100151 by Universiteit Antwerpen, Wiley Online Library on [23/12/2022]. See the Terms and Conditions (https://onlinelibrary.wiley.com/terms-and-conditions) on Wiley Online Library for rules of use; OA articles are governed by the applicable Creative Commons License

treatment time, and treatment energy influence the generation of chemical species by DBD plasma in 50 μl of PBS. H_2O_2 was measured using a fluorometric assay kit, and NO_2^- and NO_3^- were measured using the Griess method and a nitrate reductase enzyme and cofactor.

First, the treatment time was fixed to 10 s and pulsed-DBD plasma was applied using a range of pulse frequencies (50, 100, 200, and 500 Hz), which correspond to 0.9, 1.9, 3.8, and 9.4 J treatment, respectively. Unsurprisingly, as the pulse frequency (and subsequently treatment energy) increased, H_2O_2, NO_2^-, and NO_3^- concentrations increased linearly. The H_2O_2 concentration increased linearly ($R^2 = 0.85$) up to 17.1 μM for the 500 Hz (9.4 J) treatment (Figure 4a). NO_2^- and NO_3^- concentrations also increased similarly up to 42.8 and 69.4 μM for the 500 Hz treatment, respectively (Figure 4b,c).

Next, to test the sole influence of treatment time on RONS generation, pulse frequency was fixed at either 50 or 500 Hz, and plasma was applied over a range of treatment times (1, 5, 10, 50, and 100 s). H_2O_2 concentrations for both 50 and 500 Hz increased linearly ($R^2 = 0.91$ and $R^2 = 0.99$, respectively) over time (Figure 4d). Similarly, the NO_2^- and NO_3^- concentration showed a linear increase with increasing treatment time for both pulse frequencies tested (Figure 4e,f). Therefore, within the range of pulse frequencies tested (and commonly used in biomedical applications), RONS concentrations increase linearly over time.

On the basis of these results, it appeared that plasma treatment energy was also responsible for the generation of RONS. In fact, Figure 4a–c could be represented as a linear increase in plasma treatment energy (Figure 5a–c). To investigate this further, four frequencies were tested (50, 100, 200, and 500 Hz) and the treatment time was adjusted to deliver the same number of pulses (5000 pulses) during the DBD plasma treatment, corresponding to 9.4 J treatment. Following all treatments, the H_2O_2 concentration was nearly equivalent (20.18 ± 7.9 μM), regardless of the pulse frequency or the treatment time (Figure 5d). The concentrations of NO_2^- (34.2 ± 8.7 μM) and NO_3^- (82.8 ± 15.4 μM) were also nearly equivalent when the NTP treatment energy was standardized (Figure 5e,f).

Altogether, it is clear that for the DBD plasma-generated species measured here, neither pulse frequency nor application time alone was the major contributing parameter. Instead, the generation of RONS depended on the total delivered energy during treatment. This was also demonstrated with a second pulsed-DBD power supply when a fixed number of pulses was delivered at a 1-mm treatment distance. In addition to the persistent RONS measured here (H_2O_2, NO_2^-, and NO_3^-), short-lived RONS ($O/^1O_2/O_3$ and $ONOO^-$) were also analyzed following treatment. The concentrations of all these chemical species were equivalent when the total delivered energy was the same (Figure 6), suggesting that this could be used as an internal calibration for pulsed-DBD devices and RONS generation. A detailed reporting of the methods and results of this second power supply is provided in Section S4.

4 | DISCUSSION

Research into the therapeutic properties of non-equilibrium, atmospheric pressure plasma is ongoing and covers a broad range of applications. However, the ability to quantify, predict, and control plasma treatment outcomes remains a challenge and a major obstacle for clinical translation. The sensitivity of plasma to its intrinsic characteristics (e.g., voltage and waveform), application parameters (e.g., pulse frequency, time, and working distance), and environmental perturbations (e.g., gas composition, humidity, and biological surface) also contribute to the complexity of this challenge. To streamline the adoption of plasma technologies into the clinic, it is necessary to provide a method of standardizing treatment in a way that accounts for these different influences and results in a controllable and predictable therapeutic outcome. In this study, we investigated how application parameters could be standardized. We hypothesized that the delivered plasma energy encompasses the major application parameters for DBD plasma treatment and dictates biological responses.

We tested our hypothesis through electrical characterization of a microsecond-pulsed DBD system (in a pulse range commonly used in vivo and in the clinic) and by determining the energy dependence for generating chemical species and biological responses. Contrary to previous notions, we demonstrated that increasing treatment time alone does not lead to a more pronounced biological response, as other factors also play a role (Figures 2e and 3). We have summarized the parameters tested and the resulting effects on cell survival when treatment was fixed at 9.4 J (Table 2). Regardless of the treatment distance, exposure time, and pulse frequency, when cells were treated with 9.4 J of NTP, similar effects on cell viability were achieved. Here, we would like to emphasize that, while we do not believe treatment energy to be the single decisive factor for the biological response, it does encompass many of the application parameters (Table 1), thus making it a suitable candidate for further dose standardization development.

The pulsed-DBD system was operated at atmospheric pressure and in air, which is mainly composed of 78% nitrogen and 21% oxygen. In the past, it has been

16128869, 2022, 3, Downloaded from https://onlinelibrary.wiley.com/doi/10.1002/ppap.202100151 by Universiteit Antwerpen, Wiley Online Library on [23/12/2022]. See the Terms and Conditions (https://onlinelibrary.wiley.com/terms-and-conditions) on Wiley Online Library for rules of use; OA articles are governed by the applicable Creative Commons License

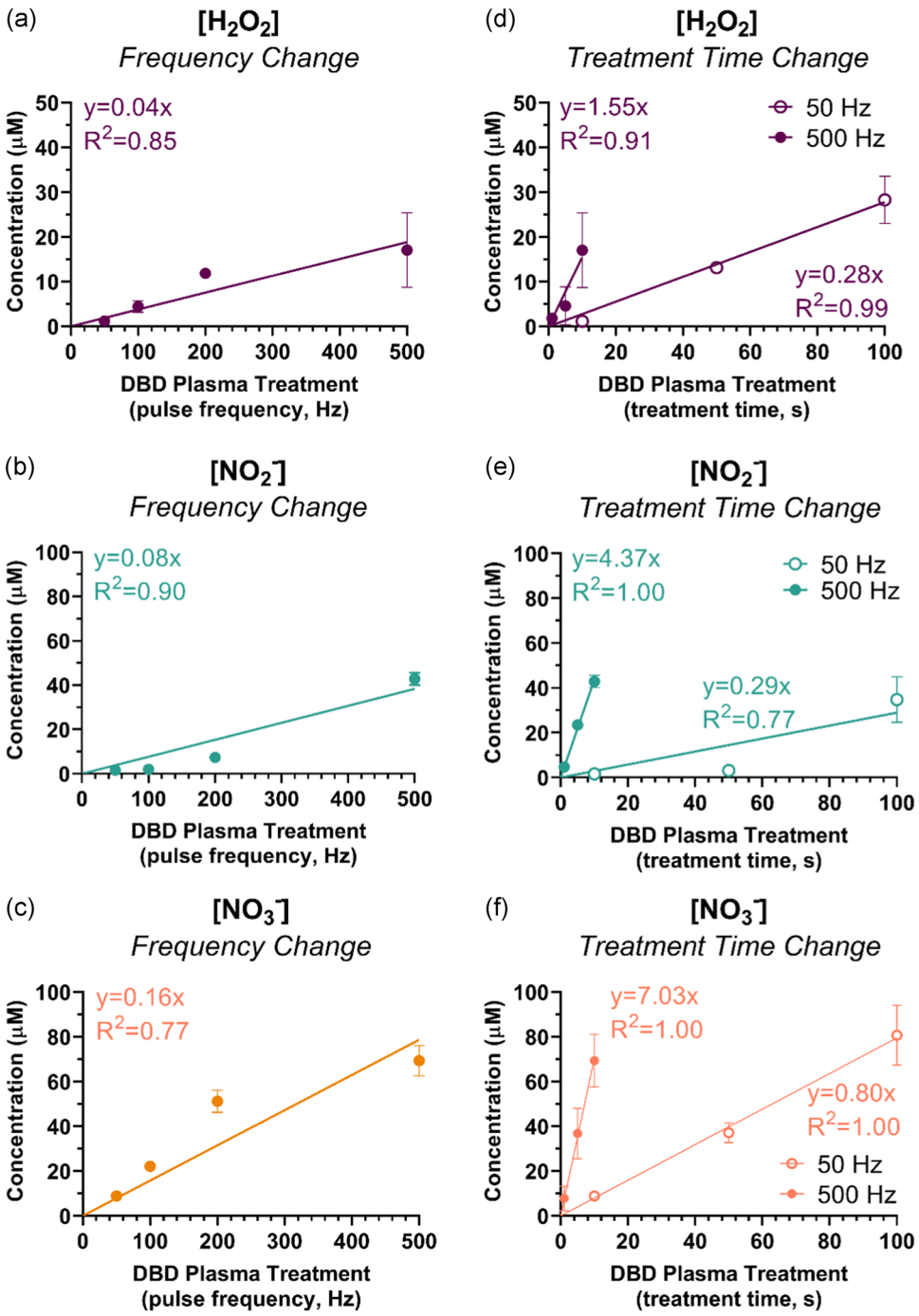


FIGURE 4 Reactive oxygen and nitrogen species concentration increased linearly with pulsed- DBD plasma treatment. Treatment was fixed at a distance of 1 mm for 10 s and a range of pulse frequencies was tested. (a) H_2O_2, (b) NO_2^-, and (c) NO_3^- concentrations were measured in phosphate-buffered saline immediately following treatment. Next, two pulse frequencies were chosen and the treatment time was adjusted. The (d) H_2O_2, (e) NO_2^-, and (f) NO_3^- concentrations increased linearly with the treatment time for both pulse frequency conditions. Data are represented here as mean ± SD ($n = 3$–9)

reported that the oxygen molecules in the air are the main effectors for both reducing cell survival and increasing cancer immunogenicity.[13,21] When air was flushed out and replaced with pure oxygen during in vitro treatment of different cell types, cell death and even immunogenic cell death were equivalent to those treated in air. When pulsed-DBD treatment was performed in pure nitrogen, no differences were observed compared to the controls. Taken together, this suggests that while DBD treatments are influenced by gas composition, they are not as sensitive as plasma jets and a minimum threshold of oxygen molecules is needed to

16128869, 2022, 3, Downloaded from https://onlinelibrary.wiley.com/doi/10.1002/ppap.202100151 by Universiteit Antwerpen, Wiley Online Library on [23/12/2022]. See the Terms and Conditions (https://onlinelibrary.wiley.com/terms-and-conditions) on Wiley Online Library for rules of use; OA articles are governed by the applicable Creative Commons License

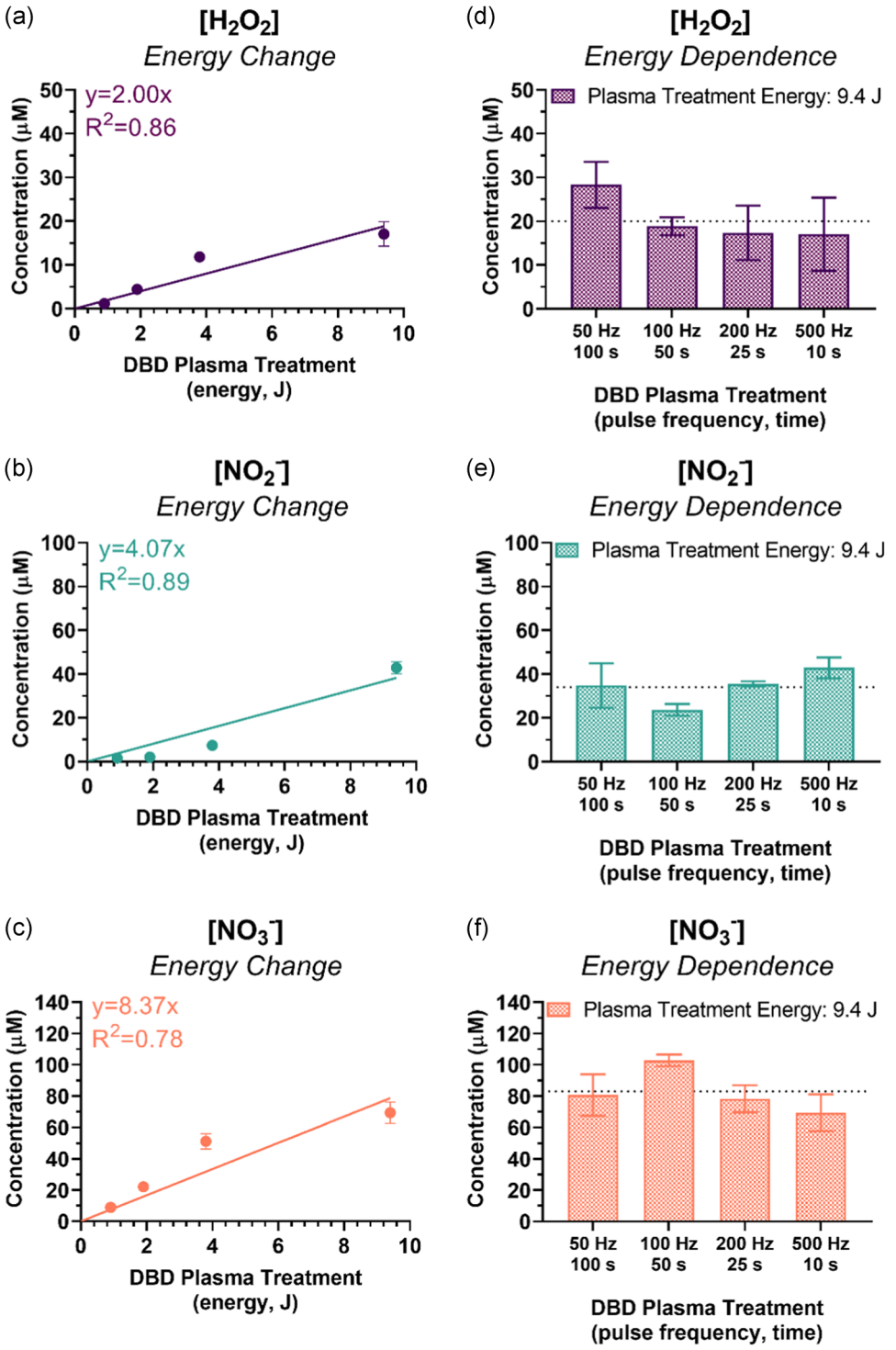


FIGURE 5 Energy dependence of the pulsed-DBD plasma treatment on reactive oxygen and nitrogen species generation. (a) H_2O_2, (b) NO_2^-, and (c) NO_3^- concentrations increased linearly in phosphate-buffered saline when exposed to plasma at higher treatment energies. Regardless of the pulse frequency or treatment time alone, when the total number of pulses was fixed, DBD plasma treatment produced nearly equivalent amounts of (d) H_2O_2, (e) NO_2^-, and (f) NO_3^-. Data are represented here as mean ± SD ($n = 3–9$) and the dotted line represents the mean concentration

16128869, 2022, 3, Downloaded from https://onlinelibrary.wiley.com/doi/10.1002/ppap.202100151 by Universiteit Antwerpen, Wiley Online Library on [23/12/2022]. See the Terms and Conditions (https://onlinelibrary.wiley.com/terms-and-conditions) on Wiley Online Library for rules of use; OA articles are governed by the applicable Creative Commons License

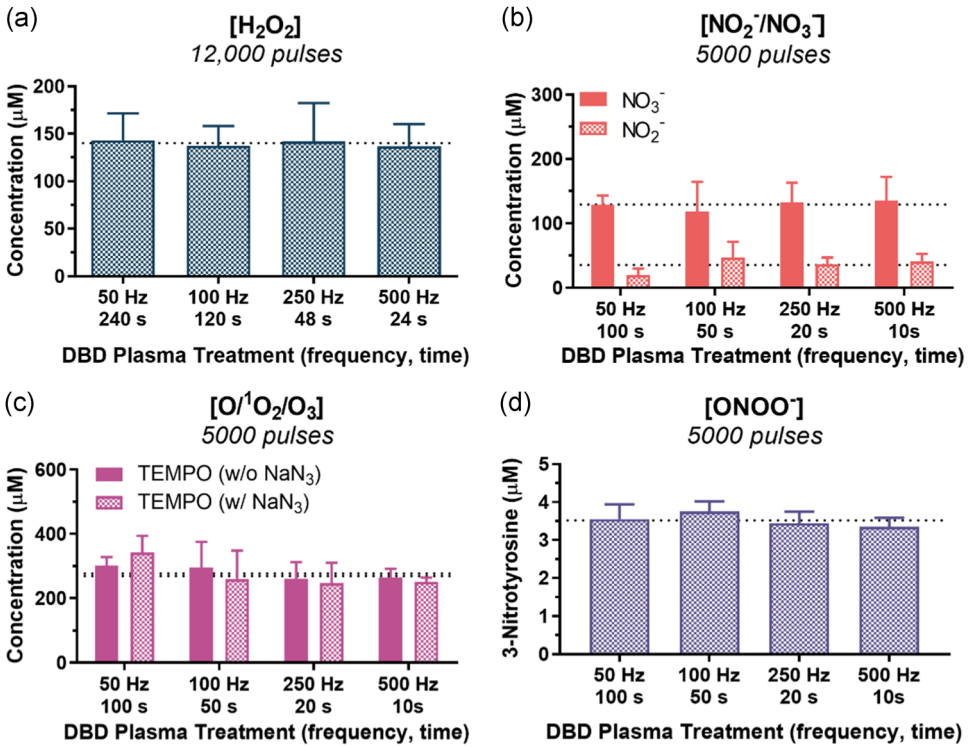


FIGURE 6 Chemical analysis of a second pulsed-DBD plasma system. Phosphate-buffered saline was treated in 24-well plates with equivalent DBD plasma treatment energy by delivering a fixed total number of pulses while pulse frequency and treatment duration were adjusted. (a) H_2O_2 concentration ($n = 3$–4) and (b) NO_2^-/NO_3^- concentration ($n = 4$–6) were measured by spectrophotometry. (c) The $O/_1O^2/O_3$ concentration ($n = 3$–5) was measured by electron paramagnetic resonance spectrometry, and (d) the $ONOO^-$ concentration ($n = 3$) was measured by liquid chromatography–mass spectrometry. Regardless of the pulse frequency or treatment time alone, when the total number of pulses, and thus treatment energy, was fixed, pulsed-DBD plasma treatment produced equivalent amounts of all reactive oxygen and nitrogen species measured here. Data are represented as mean ± SD and the dotted line represents the mean concentration

TABLE 2 Treatment of cells at an equivalent total nonthermal plasma (NTP) energy resulted in similar cell viability, independent of a single parameter

Total NTP treatment energy (J)	Treatment distance (mm)	Treatment time (s)	Pulse frequency (Hz)	Delivered pulses (Pulses)	A375 viability (%)	Cal-27 viability (%)	U87 viability (%)
9.4	1	10	500	5000	52 ± 6	61 ± 8	63 ± 3
	1	50	100	5000	48 ± 4	64 ± 6	62 ± 4
	1	100	50	5000	44 ± 2	50 ± 9	60 ± 8
9.4	1	10	500	5000	57 ± 4	59 ± 3	59 ± 3
	5	13	500	6500	70 ± 6	73 ± 5	60 ± 8
	7	30	500	15 000	70 ± 5	61 ± 6	56 ± 9
	10	41	500	20 500	67 ± 4	68 ± 3	56 ± 7

achieve a biological response. Furthermore, as the composition of air remains relatively the same and in the clinical context, hospital settings are further controlled, marked changes to air composition that would affect DBD treatment (and associated changes to discharge energy) seem unlikely.

It has been reported that the surface of treatment can greatly affect plasma discharge.[13,28] Lin et al.[13] and Simoncelli et al.[28] have shown that electrical power is higher for plasma discharges on metal compared to a dielectric for both DBDs and plasma jets, respectively. As plasma treatments in this study for all chemical and

16128869, 2022, 3, Downloaded from https://onlinelibrary.wiley.com/doi/10.1002/ppap.202100151 by Universiteit Antwerpen, Wiley Online Library on [23/12/2022]. See the Terms and Conditions (https://onlinelibrary.wiley.com/terms-and-conditions) on Wiley Online Library for rules of use; OA articles are governed by the applicable Creative Commons License

biological analyses were performed in polystyrene well plates, the energy per pulse of DBD plasma was calculated in a setting that closely resembles these experiments (Figure 1). Furthermore, we demonstrated that as the application distance of plasma treatment was increased, the energy per pulse was reduced (Figure 2c). DBD plasma treatment of three human cancer cell lines also revealed the same trend in cell survival (Figure 2d), though no statistically significant differences were observed at relatively small distances (1–3 mm). While these small changes in distance may affect the aqueous species generated, they did not significantly affect biological response. Furthermore, we demonstrated that equivalent cell survival could be achieved following NTP treatment of the cell lines at various distances if the treatment time was also adjusted to deliver the same energy (Figure 3). Interestingly, this shows that treatment is not limited to short distances, as long as the total treatment energy required for a biological response can be delivered. Taken together, this suggests that the plasma treatment energy also accounts for the working distance parameter.

We recognize several limitations of our study, mainly due to the limitations of our power supply. As the voltage and waveform of the power supply could not be changed, we were unable to test how these could affect treatment energy and subsequent chemical and biological responses. When looking into previous reports where the energy of in vitro treatment was defined, we see that these parameters indeed contribute to the measured energy per pulse.[20,35,36] Therefore, it may be that as pulsed-DBD systems transition into the clinic, the plasma treatment range must be standardized for each device. Furthermore, it would be of interest to investigate how the discharge develops in the different systems, with varying treatment parameters, while keeping the total delivered energy constant. Indeed, we have identified similar trends in a separate microsecond-pulsed DBD power supply on the biological response (Figure S3) and the generation of RONS (Figure 6), but more, in-depth investigation needs to be conducted and broad applicability still must be tested. Furthermore, future translation of plasma technology might need to consider the area or mass of the treatment target, similar to how radiotherapy doses are defined today. However, taken together, this provides insight into how pulsed-DBD plasma treatment energy could be used to standardize plasma therapy for cancer applications.

Progress toward standardizing the plasma treatment dose is critically needed for wide clinical adoption of plasma medicine technologies and work toward a plasma treatment unit has also been proposed.[37] Recently, Cheng et al.[38] have also suggested an equivalent total oxidation potential (ETOP) as a means to summarize plasma treatment dose. In this paper, the authors have provided an equation that relies on several factors including oxidation potential of various species, average number density and velocity of the species, cross-section of plasma interaction area, and treatment time. They have correlated this ETOP to bacterial reduction for several plasma jets, but further practical and clinical considerations are still required, including how the application parameters affect ETOP.

Still another challenge that must be addressed to overcome this barrier for clinical adoption includes the reproducibility of treatment. Current devices in the clinic are handheld and operated by the clinician and, therefore, rely heavily on the clinician's judgment.[3,4,32,32,39–43] Consequently, this leads to a large variability, which is further amplified when the ratio of the treatment area to the plasma applicator is large and the plasma applicator must be translated across the field for complete treatment. These challenges are not exclusive to plasma treatment and have also been faced by radiation technology.[44–46] Therefore, implementation of solutions from radiotherapy could also greatly benefit plasma technology. For example, real-time tumor tracking is a recent methodology that actively counteracts tumor wandering with compensatory motion of the source or the target.[44,47] Gidon et al.[17] and Bonzanini et al.[48,49] have also investigated the use of machine learning and nonlinear model-predictive control strategies to deliver a safe plasma dose. They have aimed to quantify thermal dose and temperature changes on the plasma-treated surface and it would be interesting to combine their work with the insight gained from our studies presented here. In fact, in situ measurement of deposited plasma treatment energy onto target cells or patient tissue with a feedback loop control system would be highly valuable and it is of high priority in our plan to bridge the gaps between preclinical and clinical studies.

In summary, we have demonstrated that the plasma treatment energy highly influenced RONS production and biological effect for in vitro cancer application. This suggests that plasma treatment energy encompasses the impact of application parameters and warrants keen attention during translation of plasma medicine technologies. Still, more in-depth investigations into the energy dependency of DBD plasma treatment on other cancer-associated effects (e.g., type of cell death, senescence, and epithelial-to-mesenchymal transition) are needed, as well as in vivo testing. However, overall, this study aids in taking a vital step toward defining a plasma treatment unit and treatment dose, and these principles should also be investigated for other biomedical and therapeutic applications in plasma medicine as well (e.g., wound healing, neuroregeneration, and surface sterilization).

16128869, 2022, 3, Downloaded from https://onlinelibrary.wiley.com/doi/10.1002/ppap.202100151 by Universiteit Antwerpen, Wiley Online Library on [23/12/2022]. See the Terms and Conditions (https://onlinelibrary.wiley.com/terms-and-conditions) on Wiley Online Library for rules of use; OA articles are governed by the applicable Creative Commons License

ACKNOWLEDGMENTS

The authors would like to thank Karel Venken for his expertise and experience with the measurements of voltage and current profiles of plasma. They would like to thank Prof. Dr. Filip Lemière and Prof. Dr. Paul Cos for sharing their equipment. Finally, they would also like to thank Prof. Dr. Erik Fransen (StatUa Center for Statistics, University of Antwerp) for his help with the statistical analysis. This study was funded in part by the Flanders Research Foundation (12S9218N, 12S9221N, and G044420N).

CONFLICT OF INTERESTS

The authors declare that there are no conflict of interests.

DATA AVAILABILITY STATEMENT

The data that support the findings of this study are available from the corresponding author upon reasonable request.

ORCID

Abraham Lin http://orcid.org/0000-0003-0097-3323

REFERENCES

[1] M. Ueda, D. Yamagami, K. Watanabe, A. Mori, H. Kimura, K. Sano, H. Saji, K. Ishikawa, M. Hori, H. Sakakita, *Polymers* **2015**, *12*, 1338.
[2] K. Miyamoto, S. Ikehara, H. Sakakita, Y. Ikehara, *J. Clin. Biochem. Nutr. Food Sci.* **2017**, *60*, 25.
[3] G. Isbary, J. Heinlin, T. Shimizu, J. Zimmermann, G. Morfill, H. U. Schmidt, R. Monetti, B. Steffes, W. Bunk, Y. Li, *Br. J. Dermatol.* **2012**, *167*, 404.
[4] S. Bekeschus, A. Schmidt, K.-D. Weltmann, T. von Woedtke, *Medicine* **2016**, *4*, 19.
[5] A. C. Borges, K. G. Kostov, R. S. Pessoa, G. M. A. de Abreu, G. de M. G. Lima, L. W. Figueira, C. Y. Koga-Ito, *Appl. Sci.* **2021**, *11*, 1975.
[6] O. N. O'Connor, S. Cahill, S. Daniels, H. Galvin, *J. Hosp. Infect.* **2014**, *88*, 59.
[7] S. Mitra, N. Kaushik, I. S. Moon, E. H. Choi, N. K. Kaushik, *Biomedicines* **2020**, *8*, 348.
[8] K. S. Katiyar, A. Lin, A. Fridman, C. E. Keating, D. K. Cullen, V. Miller, *Appl. Sci.* **2019**, *9*, 3747.
[9] M. Keidar, D. Yan, I. I. Beilis, B. Trink, J. H. Sherman, *Trends Biotechnol.* **2018**, *36*, 586.
[10] A. M. Hirst, F. M. Frame, M. Arya, N. J. Maitland, D. O'Connell, *Tumor Biol.* **2016**, *37*(6), 1.
[11] M. Khalili, L. Daniels, A. Lin, F. C. Krebs, A. E. Snook, S. Bekeschus, W. B. Bowne, V. Miller, *J. Phys. D: Appl. Phys.* **2019**, *52*, 423001.
[12] M. H. Ngo Thi, P. L. Shao, J. D. Liao, C. C. K. Lin, H. K. Yip, *Plasma Processes Polym.* **2014**, *11*, 1076.
[13] A. Lin, N. Chernets, J. Han, Y. Alicea, D. Dobrynin, G. Fridman, T. A. Freeman, A. Fridman, V. Miller, *Plasma Processes Polym.* **2015**, *12*, 1117.
[14] S. Bekeschus, K. Wende, M. M. Hefny, K. Rödder, H. Jablonowski, A. Schmidt, T. von Woedtke, K.-D. Weltmann, J. Benedikt, *Sci. Rep.* **2017**, *7*(1), 1.
[15] X. Lu, G. Naidis, M. Laroussi, S. Reuter, D. Graves, K. Ostrikov, *Phys. Rep.* **2016**, *630*, 1. doi:10.1016/j.physrep.2016.03.003
[16] A. Privat-Maldonado, A. Schmidt, A. Lin, K.-D. Weltmann, K. Wende, A. Bogaerts, S. Bekeschus, *Oxid. Med. Cell. Longev.* **2019**, *2019*, 9062098.
[17] D. Gidon, D. B. Graves, A. Mesbah, *Plasma Sources Sci. Technol.* **2017**, *26*, 085005.
[18] X. Lu, M. Laroussi, V. Puech, *Plasma Sources Sci. Technol.* **2012**, *21*, 034005.
[19] A. Fridman, A. Chirokov, A. Gutsol, *J. Phys. D: Appl. Phys.* **2005**, *38*, R1.
[20] S. Bekeschus, A. Lin, A. Fridman, K. Wende, K.-D. Weltmann, V. Miller, A. Comparison, *Plasma Chem. Plasma Process.* **2018**, *38*(1), 1.
[21] A., Lin, B., Truong, S., Patel, N., Kaushik, E. H., Choi, G., Fridman, A., Fridman, V., Miller, *Int. J. Mol. Sci.* **2017**, *18*, 966.
[22] S. Reuter, T. von Woedtke, K.-D. Weltmann, *J. Phys. D: Appl. Phys.* **2018**, *51*, 233001.
[23] D. Dobrynin, G. Fridman, G. Friedman, A. Fridman, *New J. Phys.* **2009**, *11*, 115020.
[24] A. Lin, Y. Gorbanev, J. De Backer, J. Van Loenhout, W. Van Boxem, F. Lemière, P. Cos, S. Dewilde, E. Smits, A. Bogaerts, *Adv. Sci.* **2019**, *6*, 1802062.
[25] L. Galluzzi, A. Buqué, O. Kepp, L. Zitvogel, G. Kroemer, *Nat. Rev. Immunol.* **2016**.
[26] A. Lin, J. Razzokov, H. Verswyvel, A. Privat-Maldonado, J. de Backer, M. Yusupov, E. Cardenas de la Hoz, P. Ponsaerts, E. Smits, A. Bogaerts, *Cancers* **2021**, *13*, 579.
[27] A. Lin, E. Biscop, C. Breen, S. J. Butler, E. Smits, A. Bogaerts, *Oxid. Med. Cell. Longev.* **2020**, *2020*.9750206. doi:10.1155/2020/9750206
[28] E. Simoncelli, A. Stancampiano, M. Boselli, M. Gherardi, V. Colombo, *Plasma* **2019**, *2*, 369.
[29] A. G. Lin, B. Xiang, D. J. Merlino, T. R. Baybutt, J. Sahu, A. Fridman, A. E. Snook, V. Miller, *Oncoimmunology* **2018**, *7*, e1484978.
[30] M. Vandamme, E. Robert, S. Lerondel, V. Sarron, D. Ries, S. Dozias, J. Sobilo, D. Gosset, C. Kieda, B. Legrain, *Int. J. Cancer* **2012**, *130*, 2185.
[31] N. Chernets, D. S. Kurpad, V. Alexeev, D. B. Rodrigues, T. A. Freeman, *Plasma Processes Polym.* **2015**, *12*, 1400.
[32] P. Friedman, V. Miller, G. Fridman, A. Lin, A. Fridman, *J. Am. Acad. Dermatol.* **2017**, *76*, 352.
[33] P. Friedman, V. Miller, G. Fridman, A. J. C. Fridman, *Clin. Exp. Dermatol.* **2019**, *44*, 459.
[34] P. C. Friedman, G. Fridman, A. Fridman, *Pediatr. Dermatol.* **2020**, *37*, 706.
[35] S. Kalghatgi, G. Friedman, A. Fridman, A. M. Clyne, *Ann. Biomed. Eng.* **2010**, *38*, 748.
[36] K. P. Arjunan, G. Friedman, A. Fridman, A. M. Clyne, *J. R. Soc., Interface* **2011**, rsif20110220.
[37] A. A. Fridman, A. Lin, V. Miller, S. Bekeschus, K. Wende, K.-D. Weltmann, *Plasma Med.* **2018**, *8*, 195.
[38] H. Cheng, J. Xu, X. Li, D. Liu, X. Lu, *Phys.Plasmas* **2020**, *27*, 063514.
[39] S. G. Joshi, M. Paff, G. Friedman, G. Fridman, A. Fridman, A. D. Brooks, *Am. J. Infect. Control* **2010**, *38*, 293.
[40] H.-R. Metelmann, D. S. Nedrelow, C. Seebauer, M. Schuster, T. von Woedtke, K.-D. Weltmann, S. Kindler, P. H. Metelmann,

16128869, 2022, 3, Downloaded from https://onlinelibrary.wiley.com/doi/10.1002/ppap.202100151 by Universiteit Antwerpen, Wiley Online Library on [23/12/2022]. See the Terms and Conditions (https://onlinelibrary.wiley.com/terms-and-conditions) on Wiley Online Library for rules of use; OA articles are governed by the applicable Creative Commons License

S. E. Finkelstein, D. D. von Hoff, F. Podmelle, *Clin. Plasma Med.* **2015**, *3*, 17.
[41] S. Vandersee, *J. Wound Care* **2015**, *24*, 196.
[42] M. Schuster, C. Seebauer, R. Rutkowski, A. Hauschild, F. Podmelle, C. Metelmann, B. Metelmann, T. von Woedtke, S. Hasse, K.-D. Weltmann, *J. Cranio-Maxillofac. Surg.* **2016**, *44*, 1445.
[43] H.-R. Metelmann, C. Seebauer, V. Miller, A. Fridman, G. Bauer, D. B. Graves, J.-M. Pouvesle, R. Rutkowski, M. Schuster, S. Bekeschus, *Clin. Plasma Med.* **2018**, *9*, 6.
[44] S. H. Benedict, K. M. Yenice, D. Followill, J. M. Galvin, W. Hinson, B. Kavanagh, P. Keall, M. Lovelock, S. Meeks, L. Papiez, *Med. Phys.* **2010**, *37*, 4078.
[45] T. Depuydt, K. Poels, D. Verellen, B. Engels, C. Collen, C. Haverbeke, T. Gevaert, N. Buls, G. Van Gompel, T. Reynders, *Radiother. Oncol.* **2013**, *106*, 236.
[46] C. M. Ionescu, C. Copot, D. Verellen, *Acta Astronaut.* **2017**, *132*, 59.
[47] S. Sayeh, J. Wang, W. T. Main, W. Kilby, C. R. Maurer, *Treating Tumors that Move with Respiration*. (Eds:J. J. Kresl) J. D. Luketich) L. Papiez) R. A. Schulz, R. D. Timmerman) Springer, Berlin Heidelberg, Germany **2007**, p. 15.
[48] A. D. Bonzanini, J. A. Paulson, D. B. Graves, A. Mesbah, Bonzanini Angelo D., Paulson Joel A., Makrygiorgos Georgios & Mesbah Ali Computers & Chemical Engineering 2021, 145, 107174. doi:10.1016/j.compchemeng.2020.107174
[49] A. D. Bonzanini, K. Shao, A. Stancampiano, D. B. Graves, A. Mesbah, *IEEE Trans. Radiat. Plasma Med. Sci.* **2021**, 1. doi:10.1109/TRPMS.2021.3055727

SUPPORTING INFORMATION

Additional supporting information may be found in the online version of the article at the publisher's website.

How to cite this article: A. Lin, E. Biscop, Y. Gorbanev, E. Smits, A. Bogaerts. Toward defining plasma treatment dose: The role of plasma treatment energy of pulsed-dielectric barrier discharge in dictating in vitro biological responses. *Plasma Processes Polym.* **2022**;19:e2100151. doi:10.1002/ppap.202100151

16128869, 2022, 3, Downloaded from https://onlinelibrary.wiley.com/doi/10.1002/ppap.202100151 by Universiteit Antwerpen, Wiley Online Library on [23/12/2022]. See the Terms and Conditions (https://onlinelibrary.wiley.com/terms-and-conditions) on Wiley Online Library for rules of use; OA articles are governed by the applicable Creative Commons License